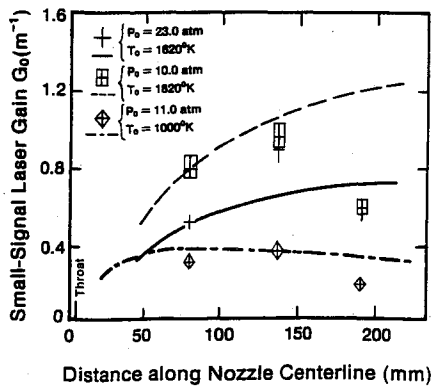

Fig. 3 Comparison between theoretical (lines) and experimental (points) small-signal laser gain profiles.

Conclusions

Small-signal gain measurements were conducted in a shock tube driven nonequilibrium expansion of a gas mixture containing 6.6% CO_2, 54.1% N_2, and 39.3% He at different reservoir conditions. The gain measurements were made at three locations downstream from the nozzle throat of a long double-wedge type hypersonic nozzle. The experimental results were compared with computer code predictions. The main results of this investigation are as follows:

1) Good agreement between the experimental data and the analytical predictions for the small-signal gain was obtained at the two stations closer to the nozzle throat.

2) Poor agreement between the experimental data and theoretical predictions for gain occurred at the station near the nozzle exit. At that location, the analytical model overestimates the actual gain. A possible reason could be the underestimation of the deactivation rate used by the theory.

3) Small-signal gain peaks of 0.9 m^{-1}, comparable with those obtained in minimum length contoured nozzles, were measured.

Acknowledgments

The authors wish to express their appreciation to the Brazilian Air Force for funding the present work. Particularly to Air Force Colonel Reginaldo dos Santos, director of the Instituto de Estudos Avançados, for his support and encouragement throughout this project. Thanks also to Sylvio Fish de Miranda for his valuable help at the laboratory during the tests. Acknowledgment is also due to Henry T. Nagamatsu and Leik N. Myrabo, from Rensselaer Polytechnic Institute, for their extremely useful advice and suggestions during the review of this work.

References

[1]Anderson, J. D., Jr., *Gasdynamic Lasers: An Introduction,* Chap. 5, Appendix A, Academic, New York, 1976.

[2]Lee, G., "Quasi-One-Dimensional Solution for the Power of CO_2 Gasdynamic Lasers," *Journal of Physics of Fluids,* Vol. 17, No. 3, 1974, pp. 644-649.

[3]Anderson, J. D., Jr., Humphrey, R. L., Vamos, J. S., Plummer, M. J., and Jensen, R. E., "Population Inversions in an Expanding Gas: Theory and Experiment," Naval Ordnance Lab., White Oak, MD, NOLTR 71-116, 1971.

[4]Mitra, N. K., and Fiebig, M., "Viscous Nozzle Flows and CO_2 Gasdynamic Lasers," *Proceedings of the International Symposium on Gasdynamic and Chemical Lasers,* DFVLR Press, Köln, Germany, Oct. 1976, pp. 298-340.

[5]Buonadona, V. R., and Christiansen, W. R., "Gain Measurements of High Temperature CO_2 Laser Mixtures in Shock Tube Driven Flow," *Recent Developments in Shock Tube Research,* Stanford Univ. Press, Stanford, CA, 1973, pp. 174-183.

[6]Klosterman, E. L., and Hoffman, A. L., "A High Pressure Shock Tube Driven Gasdynamic Laser," *Recent Developments in Shock Tube Research,* Stanford Univ. Press, Stanford, CA, 1973, pp. 156-166.

[7]Nagamatsu, H. T., Geiger, R. E., and Sheer, R. E., Jr., "Hypersonic Shock Tunnel," *ARS Journal,* Vol. 29, May 1959, pp. 332-340.

[8]Glowacki, W. J., and Anderson, J. D., Jr., "A Computer Program for CO_2-N_2-H_2O Gasdynamic Laser Gain and Maximum Available Power," Naval Ordnance Lab., White Oak, MD, NOLTR 71-210, 1971.

[9]Minucci, M. A. S., "Gain Measurements in a CO_2 CW Gas Dynamic Laser," M. Sc. Thesis, Inst. Tecnológico de Aeronáutica, Dept. of Aeronautical Engineering, S. J. dos Campos, São Paulo, Brazil, Dec. 1986 (in Portuguese).

[10]Minucci, M. A. S., and Hinckel, J. N., "Laser Gain Profiles During the Nonequilibrium Expansion of a CO_2-N_2-He System Through a Long Double-Wedge Type Hypersonic Nozzle," AIAA Paper 90-1511, June 1990.

Derivation and Testing of a One-Equation Model Based on Two Time Scales

U. C. Goldberg*
Rockwell International Science Center, Thousand Oaks, California 91360

Introduction

TURBULENCE measurements indicate that large-scale energy generating eddies possess a development rate substantially different from that of small-scale dissipative eddies. This suggests using a model that treats these eddies separately, assigning each range its own time scale. In the present work, a one-equation model is developed wherein the velocity scale is determined from the solution of an equation for the turbulence kinetic energy and the length scale is found indirectly from two time scales assigned each to large and small eddies. The derivation of this model leads to an expression for the near-wall function f_μ used in low Reynolds number versions of the k-ϵ model. A backflow model[1] is applied in conjunction with the one-equation model for the treatment of detached flow regions. Several flow cases are calculated to test the performance of this turbulence model.

Model Formulation

To account separately for the large (energy producing) eddies and the small (dissipative) eddies, characteristic time scales are assigned to each. Thus, the large eddies are characterized by

$$t_k \sim k/\epsilon \tag{1}$$

where k is the kinetic energy of the turbulence $k = \frac{1}{2}\overline{u_i' u_i'}$, and ϵ is the dissipation rate of k.

The small eddies are characterized by the Kolmogorov scale

$$t_\epsilon \sim \sqrt{\nu/\epsilon} \tag{2}$$

where ν is the kinematic molecular viscosity.

To determine these time scales, k and ϵ must be known throughout the flowfield. In the present work k is determined from the solution of a partially modeled version of the exact equation for turbulence kinetic energy

$$\frac{\partial}{\partial t}(\rho k) + \frac{\partial}{\partial x_i}(\rho U_i k) = \frac{\partial}{\partial x_i}\left[\left(\mu + \frac{\mu_t}{\sigma_k}\right)\frac{\partial k}{\partial x_i}\right] - \rho\overline{u_i' u_j'}\frac{\partial U_i}{\partial x_j} - C_k\frac{(\rho k)^2}{\mu_t} \tag{3}$$

Received Aug. 15, 1990; revision received Sept. 10, 1990; accepted for publication Sept. 18, 1990.

*Member Technical Staff. Member AIAA.

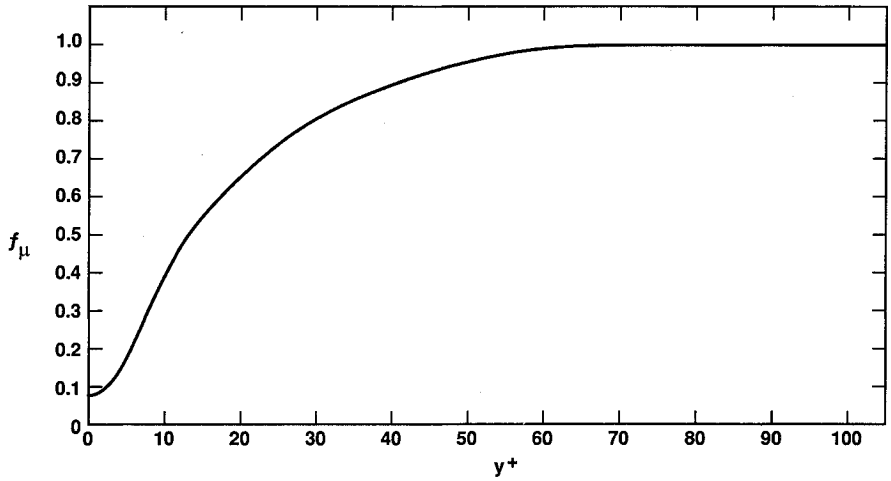

Fig. 1 Variation of $f\mu$ with distance from wall.

where ρ and μ are the fluid density and dynamic molecular viscosity, respectively, U_i and u_i' are the mean and fluctuating velocity components, respectively, t is time, x_i are the space coordinates, and μ_t is the dynamic eddy viscosity. The two constants appearing in Eq. (3) have the values $\sigma_k = 1.0$, $C_k = 0.080$, and the Reynolds stresses are related to the mean flow gradients by the Boussinesq concept

$$-\overline{\rho u_i' u_j'} = \mu_t\left[\left(\frac{\partial U_i}{\partial x_j}+\frac{\partial U_j}{\partial x_i}\right)-\frac{2}{3}\frac{\partial U_k}{\partial x_k}\delta_{ij}\right]-\frac{2}{3}\rho k\delta_{ij} \qquad (4)$$

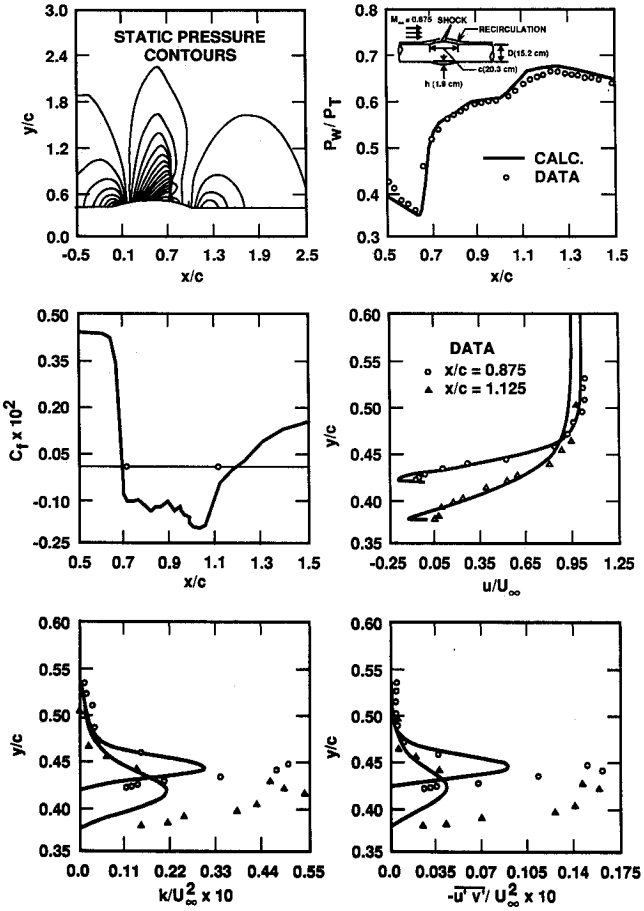

Fig. 2 Transonic flow over an axisymmetric bump.

Equations (3) and (4) are solved coupled with the μ_t field given below, subject to the following boundary and initial conditions:

1) Boundary conditions: at solid walls, $k_w = 0$; on inviscid surfaces, wakes, or symmetry surfaces $\partial k/\partial y = 0$ where y is the local normal-to-surface coordinate; at freestream inflows, $k_{in} = 10^{-6}U_\infty^2$.

2) Initial conditions: Eq. (3) has the trivial solution $k = 0$. Thus, to enable a time-marching calculation, some initial guess is necessary throughout the computational domain. A value of $k_0 = 10^{-6}U_\infty^2$ is used.

Note that ϵ is expressed algebraically in terms of k and a length scale that guarantees proper behavior from the wall to the fully turbulent region[2-4]

$$\epsilon = 2A_\epsilon k^{3/2}/[y(1-e^{-A_\epsilon R_y})] \qquad (5)$$

where $A_\epsilon = C_\mu^{3/4}/2\kappa$, $\kappa = 0.4$, $C_\mu = 0.09$, $R_y = \sqrt{k}y/\nu$.

With k and ϵ known, the two time scales, Eqs. (1) and (2) are established.

The velocity scale, needed to complete the formulation for the eddy viscosity field, is given by

$$V = \sqrt{k} \qquad (6)$$

Combining Eqs. (1), (2), and (6) yields two eddy viscosity fields, corresponding to the two time scales

$$\nu_k \sim V^2 t_k = C_\mu k^2/\epsilon \qquad (7)$$

$$\nu_\epsilon \sim V^2 t_\epsilon = C_\epsilon k\sqrt{\nu/\epsilon}\,(1-e^{-A_\mu R_y}) \qquad (8)$$

Equation (7) recovers the formula for eddy viscosity used in the high-turbulence-Reynolds number k-ϵ model.[3] In Eq. (8), a damping function was introduced to guarantee the correct behavior of eddy viscosity near solid surfaces[3] where dissipative eddies, represented by ν_ϵ, prevail. The constant $A_\mu = 0.016$ to recover the value $B = 5.5$ in the logarithmic law $u^+ = \kappa^{-1}\ln y^+ + B$. To determine the value of C_ϵ in Eq. (8), use is made of an eddy viscosity distribution[2,3] that has the correct behavior both near walls and away from walls, namely,

$$\nu_t = \kappa C_\mu^{1/4}\sqrt{k}y(1-e^{-A_\mu R_y}) \qquad (9)$$

and of the near-wall limit of Eq. (5)

$$\lim_{y\to 0}\epsilon = 2\nu k/y^2 \qquad (10)$$

Equating the near-wall limits of Eqs. (8) and (9) and using Eq. (10) yields

$$C_\epsilon = \sqrt{2}\kappa C_\mu^{1/4} \tag{11}$$

Next, the two branches of the eddy viscosity field [Eqs. (7) and (8)] are combined into one expression that has the correct limits near walls (ν_ϵ) and away from walls (ν_k). This is achieved by introducing a near-wall function

$$f_\mu = \{1 + [A_\epsilon \sqrt{k^+} y^+ (1 - e^{-A_\epsilon \sqrt{k^+} y^+})]^{-1/2}\}(1 - e^{-A_\mu \sqrt{k^+} y^+}) \tag{12}$$

where $y^+ = yu_\tau/\nu$, $k^+ = k/u_\tau^2$, and $u_\tau = \sqrt{\tau_w/\rho_w}$; thus, $\sqrt{k^+} y^+ = R_y$.

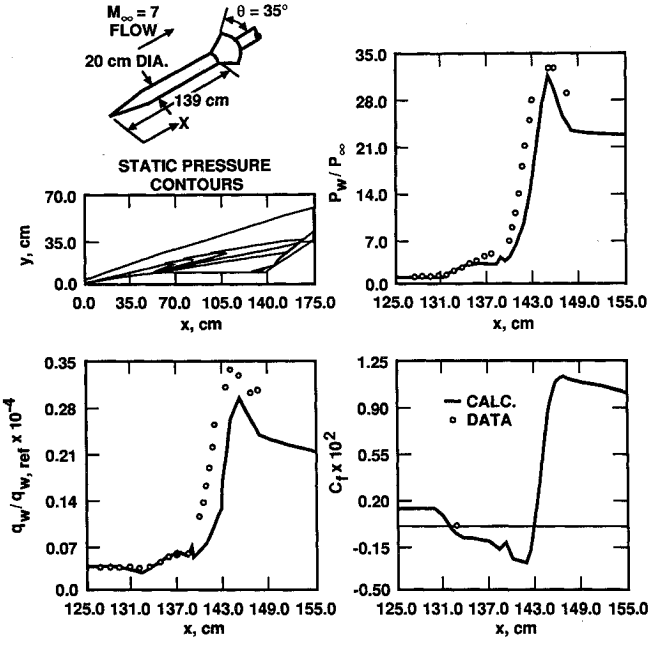

Fig. 3 Hypersonic flow over a cone-ogive-cylinder-flare configuration.

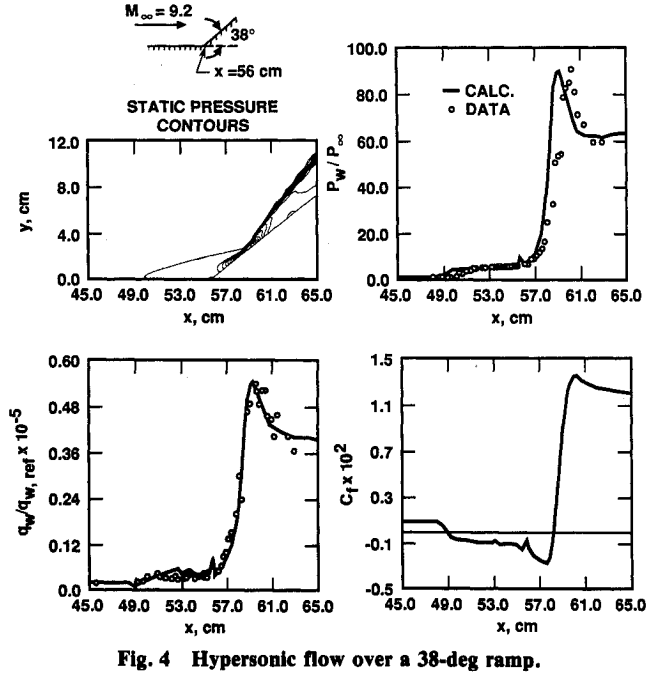

Fig. 4 Hypersonic flow over a 38-deg ramp.

It can be shown, using Eq. (5), that

$$C_\mu f_\mu \to \begin{cases} C_\mu, & R_y \gg 1 \\ A_\mu C_\epsilon R_y \sqrt{\nu\epsilon}/k, & R_y \ll 1 \end{cases}$$

so that the entire eddy viscosity field is given by the formula

$$\nu_t = C_\mu f_\mu k^2/\epsilon \tag{13}$$

It is noted that Eq. (12) serves as a near-wall function also for low Reynolds number k-ϵ models. Figure 1 shows the variation of f_μ with y.

The length scales implied by the current model formulation are derived next. Since $\nu_t = VL$, where L is the length scale, it follows from Eqs. (5-8) that the length scales corresponding to the large and small eddies, respectively, are

$$L_k = \kappa C_\mu^{1/4} y(1 - e^{-A_\epsilon R_y}) \tag{14}$$

$$L_\epsilon = \sqrt{\frac{2\kappa^3 \nu}{C_\mu^{1/4} k^{1/2}}}\, y(1 - e^{-A_\epsilon R_y})(1 - e^{-A_\mu R_y}) \tag{15}$$

From Eq. (15) it is seen that $L_\epsilon \sim (\nu y)^{1/2} k^{-1/4}$. This is in contrast with the linear behavior $L \sim y$, which is typical of conventional one-equation models.

Finally, within backflow regions, the eddy viscosity is calculated using Goldberg's backflow model.[1]

Results

Several flow test cases were computed to assess the performance of the new turbulence model, using the USA code.[5]

Case 1

An axisymmetric transonic flow over a bump[6] at $M_\infty = 0.875$ is computed. Figure 2 shows the geometry, pressure contours, comparisons for pressure, and skin friction distributions, as well as for velocity, turbulence kinetic energy, and Reynolds stress profiles at two streamwise locations.

Case 2

Flow over a cone-ogive-cylinder flare[7] at $M_\infty = 7.05$ is considered next. Figure 3 shows the geometry, pressure contours, and comparisons between the calculation and the experimental data for pressure, heat transfer, and skin friction.

Case 3

This test case is an $M_\infty = 9.2$ flow over a 38-deg two-dimensional ramp.[8] Figure 4 shows geometry, pressure contours, comparisons between the computed and experimental results for pressure and heat transfer distributions, and the predicted skin friction.

Conclusions

A one-equation turbulence model was described and its performance demonstrated through calculation of several flow cases. The formulation of the model, using two time scales, led to the derivation of an expression for the near-wall function f_μ, used in low Reynolds number versions of the k-ϵ model.

References

[1]Goldberg, U. C., "Separated Flow Treatment with a New Turbulence Model," *AIAA Journal*, Vol. 24, No. 10, 1986, pp. 1711-1713.

[2]Wolfshtein, M., "The Velocity and Temperature Distribution in One-Dimensional Flow with Turbulence Augmentation and Pressure Gradient," *International Journal of Heat and Mass Transfer*, Vol. 12, 1969, pp. 301-318.

[3]Goldberg, U. C., and Ota, D. K., "A k-ϵ Near-Wall Formulation for Separated Flows," AIAA Paper 90-1482, 1990.

[4]Goldberg, U. C., and Chakravarthy, S. R., "Separated Flow Predictions Using a Hybrid k-L/Backflow Model," *AIAA Journal*, Vol. 28, No. 6, 1990, pp. 1005–1009.

[5]Chakravarthy, S. R., Szema, K.-Y., and Haney, J. W., "Unified 'Nose-to-Tail' Computational Method for Hypersonic Vehicle Applications," AIAA Paper 88-2564, June 1988.

[6]Bachalo, W. D., and Johnson, D. A., "An Investigation of Transonic Turbulent Boundary Layer Separation Generated on an Axisymmetric Flow Model," AIAA Paper 79-1979.

[7]Kussoy, M. I., and Horstman, C. C., "Documentation of Two- and Three-Dimensional Hypersonic Shock Wave/Turbulent Boundary Layer Interaction Flows," NASA TM 101075, Jan. 1989.

[8]Coleman, G. T., and Stollery, J. L., "Heat Transfer in Hypersonic Turbulent Separated Flow," Dept. of Aeronautics, Imperial College of Science and Technology, London, Rept. 72-05, March 1972.

Simple Algebraic Technique for Nearly Orthogonal Grid Generation

S. Saha* and B. C. Basu†
Indian Institute of Technology, Kharagpur, India

I. Introduction

GRID generation is a very important aspect of solving computational fluid dynamics (CFD) problems where a set of partial differential equations has to be solved in a given domain. It is desirable for the grid to have good orthogonality properties, and the grid generator should be able to produce an arbitrary amount of clustering near the body surface when necessary. Generation of body-fitted coordinates meeting these requirements using algebraic techniques are described by Eiseman[1] and Smith.[2] It is well known that the most efficient way of dividing the domain for external flow problems is by generating an O-type grid for a two-dimensional case or an O-O topology grid for a three-dimensional case, since they give the maximum resolution near the body surface with the minimum number of grid points. A simple algebraic technique has been developed for generating an O-type grid or an O-O topology grid for a geometry with sharp edges having a high grid density near the body surface while maintaining orthogonality. The present method generates the grid by distributing spacings in the outward normal direction from a closed contour as a function of the rate of change of arc length in that direction. This procedure, when applied to subsequently generated contours, evolves a nearly orthogonal grid with a circular outer boundary. A similar procedure applied to a closed three-dimensional surface produces a spherical outer boundary, thereby generating an O-O topology grid.

II. Method

In this method, at every point on the body surface and subsequently generated constant j contours (i and j represent the wraparound and outer boundary directions, respectively), the rate of change of i-direction arc length $s(i)$ in the outward normal direction ($\mathrm{d}s(i)/\mathrm{d}n$, n being the outward normal vector) is computed. The value of $\mathrm{d}s(i)/\mathrm{d}n$ for a panel of length $s1$ is given by $(s2-s1)/d$ where $s2$ is the distance between the points obtained by moving a small distance d along the normals at the panel endpoints. The value of $\mathrm{d}s(i)/\mathrm{d}n$ at a node is taken as the average of $\mathrm{d}s(i)/\mathrm{d}n$ at neighboring panels. The distribution of maximum physical spacing between the constant j contours [i.e., $S\mathrm{max}(j)$] is prescribed. Now the spacings $S(i)$ in the normal direction are distributed such that where $\mathrm{d}s(i)/\mathrm{d}n$ is small, the spacing is large and vice versa, the maximum spacing being $S\mathrm{max}(j)$ for the particular constant j contour. The $j+1$ contour obtained by this procedure has a smoother variation of curvature or $\mathrm{d}s(i)/\mathrm{d}n$, and as j increases, the curvature tends to become equal everywhere. Thus, starting from an arbitrary body surface geometry, the outer boundary evolves as a circle and an O-type grid is generated.

Near the body surface, where there is a large difference between maximum and minimum values of $\mathrm{d}s(i)/\mathrm{d}n$, the ratio between minimum spacing $S\mathrm{min}/S\mathrm{max}$ [i.e., $S\mathrm{max}=S\mathrm{max}(j)$] is kept small (0.1, say) to smooth the variation of $\mathrm{d}s(i)/\mathrm{d}n$ rapidly. As j increases, the variation of $\mathrm{d}s(i)/\mathrm{d}n$ decreases, and $S\mathrm{min}/S\mathrm{max}$ is gradually increased to the value of unity at the outer boundary. In the present work, an exponential distribution has been considered, i.e.,

$$S\mathrm{min}/S\mathrm{max}=f\mathrm{min}+(1-f\mathrm{min})\times\exp[sr\mathrm{min}-sr\mathrm{max})c0]$$

where $f\mathrm{min}$ is the smallest value of $S\mathrm{min}/S\mathrm{max}$ for a particular grid, $sr\mathrm{min}$ and $sr\mathrm{max}$ are the minimum and maximum values of $\mathrm{d}s(i)/\mathrm{d}n$ for the particular j contour, and $c0$ is a constant.

The choice of distribution function for determination of the actual spacings $S(i)$ on a particular constant j line is not unique. The one used in the present case is an exponential distribution chosen to vary the spacings rapidly near small or negative values of $\mathrm{d}s(i)/\mathrm{d}n$, and this helps in avoiding cross over of adjacent lines by reducing the concavity of the surface very quickly. The distribution function is given by

$$S(i)=S\mathrm{min}+(S\mathrm{max}-S\mathrm{min})\times\exp[c1(sr\mathrm{min}-\mathrm{d}s(i)/\mathrm{d}n)]$$

where $S\mathrm{min}$ and $S\mathrm{max}$ refer to the maximum and minimum spacings for a particular constant j contour, $sr\,\mathrm{min}$ is the minimum value of $\mathrm{d}s(i)/\mathrm{d}n$ for that contour, and $c1$ is a constant.

When the variation in $\mathrm{d}s(i)/\mathrm{d}n$ is not very smooth, or j-direction spacings $S(i)$ are quite large compared to $s(i)$, waviness may be generated that gets amplified as j increases. To suppress this, a few smoothing sweeps are added before the final distribution of spacings is used to obtain the contour at $j+1$. The smoothing is done selectively at the points where this waviness is generated by adding a fraction (5–10%) of the second difference of $S(i)$ in the i direction. The selective smoothing is performed by excluding those points from the smoothing operation at which the newly generated contour at $j+1$ obtained with the trial spacing distribution is smoother than the previous contour, i.e., when $\mathrm{d}s(i)/\mathrm{d}n$ at both j and $j+1$ are positive and $[\mathrm{d}s(i)/\mathrm{d}n]_{j+1}<[\mathrm{d}s(i)/\mathrm{d}n]_j$, or when $\mathrm{d}s(i)/\mathrm{d}n$ at both j and $j+1$ are negative and $[\mathrm{d}s(i)/\mathrm{d}n]_{j+1}>[\mathrm{d}s(i)/\mathrm{d}n]_j$. Usually about four to six smoothing sweeps are sufficient.

The generation procedure in three dimensions is identical with the rate of change of surface area considered instead of arc length for determination of the spacings in the normal direction. For smoothing in three dimensions, the second difference is replaced by the sum of the differences in spacings of the four neighboring points with the point in question.

For calculation of direction cosines of grid lines in the radial direction at an edge of a flat plate (with zero thickness), a thickness is temporarily added at all points except those on the edge. The average of the normals on the neighboring points on the upper and lower surfaces is now taken as the direction cosine at a point on the edge after subtracting the component along the edge. The direction cosine at a corner is obtained by taking the average of the direction cosines at neighboring points on the edges meeting at the corner.

No iterations are required in the present method except for the smoothing sweeps. Other noniterative methods for grid generation, such as solution of hyperbolic partial differential equations, are equally efficient. However, with the latter approach, the slope discontinuities on the body surface are likely to be propagated into the interior grid.[3]

Received Jan. 22, 1990; revision received July 24, 1990; accepted for publication Aug. 13, 1990.

*Junior Scientific Officer, Aerospace Engineering Department.
†Professor, Aerospace Engineering Department.